The viscosity and ion conductivity of polydimethylsiloxane systems: 2. Ion concentration effects

J. E. Companik* and S. A. Bidstrup†
School of Chemical Engineering, Georgia Institute of Technology, Atlanta, GA 30332-0100, USA
(Received 23 July 1993; revised 30 March 1994)

A homologous series of polydimethylsiloxane (PDMS) oils was doped with varying amounts of PDMS salts of three different univalent cations (sodium, tetramethylammonium and tetrapropylammonium). The zero-shear-rate viscosity and ion conductivity of each sample were measured over the temperature range $-50°C < T < 60°C$. Free volume and Arrhenius type viscosity and ion conductivity models were successfully applied to these data. The effects of mobile ion concentration on the values of the best-fit model parameters were explored.

(Keywords: viscosity; ion conductivity; polydimethylsiloxane)

INTRODUCTION

The goal of this investigation is to develop a fundamental understanding of chain segment and ion mobility in polymer systems. This basic understanding includes the development of relationships between chain segment mobility (viscosity), ion mobility (ion conductivity) and changes in the polymer system (e.g. changes in molecular weight, glass transition temperature (T_g), thermal expansion coefficient, ion size and mobile ion concentration). This study has three important areas of application: the improved design and processing of polymer systems used in microelectronics encapsulation[1]; the design of better polymer/salt complexes (polymer electrolytes) for use in electrochemical devices[2]; and the potential use of ion conductivity as a means of polymer cure monitoring and control[3,4].

In this investigation, a homologous series of polydimethylsiloxane (PDMS) oils and six homologous series of PDMS salts of various univalent cations (sodium, potassium, tetramethylammonium (TMA^+), tetraethylammonium (TEA^+), tetrapropylammonium (TPA^+) and tetrabutylammonium (TBA^+)) were chosen as the model systems. PDMS oil systems were chosen for this study because they are commonly used as encapsulants in the microelectronics industry, have very low inherent ion impurity contents (below the level of detection of our dielectric analyser, $10^{-15}\,\Omega\,cm^{-1}$) and are easily characterizable over a wide temperature range. PDMS salt systems were chosen for this study because they possess physical properties similar to the oils and permit simple manipulation of both mobile cation size and mobile cation concentration (by adding different amounts of salt to the neat oil systems).

Previously[5], the effects of polymer chain length and ion size on the zero-shear-rate viscosity and ion conductivity of these PDMS systems were investigated. Free volume and Arrhenius viscosity and ion conductivity models successfully described these systems, and changes in the best-fit model parameters were found to be related to changes in mobile chain segment length and ion size.

In this study, three different chain length PDMS oils are doped with varying amounts of PDMS salts, with the same chain length, of three different univalent cations (Na^+, TMA^+ and TPA^+). The zero-shear-rate viscosity and ion conductivity of each sample are measured over the temperature range $-50°C < T < 60°C$. Free volume and Arrhenius type viscosity and ion conductivity models are applied to these data, and the effects of mobile ion concentration on the values of the best-fit model parameters are explored.

THEORETICAL BACKGROUND

Viscosity of polymer systems

As discussed in more detail in an earlier paper[5], viscous polymer flow is dependent on the characteristics of both the whole chain structure and the local chain structure. Therefore, models describing viscosity are usually developed as the product of two quantities: a structure factor and a segmental friction factor[6–8]. The structure factor is independent of temperature, reflects the length of the whole polymer chain, and assumes different expressions depending on whether or not complex chain interactions (i.e. chain entanglements) occur. The segmental friction factor is determined by the temperature of the system and the local chain structure (i.e. the fractional free volume of the system, the size of the unit of flow, and the attraction forces between chain segments). Depending on the temperature range of interest, one of two different phenomena control this segmental friction

*Current address: Motorola, Inc., Radio Products Group, 8000 W. Sunrise Blvd, Ft Lauderdale, FL 33322, USA
†To whom correspondence should be addressed

0032-3861/94/22/4834–08

factor. Therefore, a different theory of polymer flow is offered for each temperature range.

Close to the T_g ($T < T_g + 100°C$), the limiting factor for chain segment motion is the availability of sufficient free volume for a chain segment (the characteristic unit of flow) to move. In this temperature region, free volume type models (e.g. the Doolittle, Williams–Landel–Ferry (WLF) and Berry–Fox expressions) are used to describe polymer flow[4,6–13]. The Berry–Fox model is of particular interest because of the physical significance of its parameters. The free volume viscosity model applied in this research was therefore developed according to the arguments of Berry and Fox[5,6]:

$$\eta = M_w^a \zeta_0 \exp\left[\frac{B}{f_g + (\alpha_1 - \alpha_0)(T - T_g)}\right] \quad (1)$$

where η is the viscosity, M_w^a is the weight-average molecular weight of the polymer raised to the power a, ζ_0 is the inherent friction factor, B is the fractional free volume required for chain segment motion (the free volume required for a chain segment to move divided by the occupied chain segment volume), f_g is the fractional free volume at T_g, α_1 is the volumetric thermal expansion coefficient of the occupied chain segment and T is the measurement temperature.

The structure factor in equation (1) is equal to M_w^a, where $a = 1$ below the critical entanglement molecular weight (M_c) of the polymer and $a = 3.4$ above M_c[14]. The friction factor is equal to ζ_0 times the exponential term. The magnitude of ζ_0 is believed to be dependent on the local interchain and intrachain forces between neighbouring chain segments[6].

Far above T_g ($T > T_g + 100°C$), free volume availability is no longer the flow limiting factor, as sufficient free volume for segmental motion exists in the system. In this temperature range, a polymer chain segment moves from its position to an unoccupied position by overcoming an apparent activation energy. Here, Arrhenius type models are used to describe polymer flow[6–8,15–18]:

$$\eta = \eta_\infty \exp\left(\frac{E_\eta}{RT}\right) \quad (2)$$

where η_∞ is a pre-exponential factor which is a function of overall chain length (i.e. the structure factor) and E_η is the apparent activation energy for chain segment motion (i.e. the friction factor), which is related to the length of the characteristic unit of flow.

In an earlier paper[5], the free volume and Arrhenius viscosity models were shown to hold for the neat PDMS oil systems. The effects of overall polymer chain length were apparent in the structure factors of these two models, $F(Z)$ and η_∞, which both increased with overall chain length. Also, $F(Z)$ was found to equal M_w. However, a specific correlation between η_∞ and chain length for all polymers could not be made.

The effects of mobile chain segment length on viscosity in PDMS oil systems were found[5] to be reflected in the best-fit model parameters, E_η and B. Both parameters increased with mobile chain segment length, and indicated that the characteristic unit of flow in long chain PDMS molecules is close to a length of 140 main chain atoms ($M_w = 5190$). Also, f_g was found to increase with overall chain length and then level off to a constant value of 0.034 at $M_w = 5190$.

In this investigation, both the free volume (equation (1)) and Arrhenius (equation (2)) viscosity models will be applied to describe the temperature dependence of the viscosity of the PDMS salt doped PDMS oils listed in *Table 1*. In doing this, the applicability of these models to the doped oil systems will be verified. Furthermore, f_g for these systems will be determined, as the value of this parameter is necessary to apply the free volume ion conductivity model to these systems, as discussed in the next section.

Table 1 Molecular weights and glass transition temperatures of the PDMS salt doped PDMS oils used in this study, where M = TPA^+, TMA^+ or Na^+

	Oil terminal group	Salt (wt%) (balance oil)	Ions (mol%) $\times 10^3$	M_w	T_g (°C)
DM438-0.10%	Vinyl	0.10	4.76	1200	−140
DM438-0.25%	Vinyl	0.25	11.9	1200	−140
DM438-0.50%	Vinyl	0.50	23.8	1200	−140
DM438-1.00%	Vinyl	1.00	47.6	1200	−140
DM438-2.50%	Vinyl	2.50	119	1200	−140
DM438-5.00%	Vinyl	5.00	238	1200	−139
DM438-10.00%	Vinyl	10.00	476	1190	−139
DM438-100%	–	100.00	4760	1140	−124
DM039.5-0.10%	Trimethyl	0.10	2.38	2720	−127
DM039.5-0.25%	Trimethyl	0.25	5.95	2720	−127
DM039.5-0.50%	Trimethyl	0.50	11.9	2720	−127
DM039.5-0.75%	Trimethyl	0.75	17.9	2720	−127
DM039.5-1.00%	Trimethyl	1.00	23.8	2720	−127
DM039.5-1.75%	Trimethyl	1.75	41.7	2720	−127
DM039.5-100%	–	100.00	2380	2650	−126
DM441.2-0.10%	Vinyl	0.10	0.56	12800	−126
DM441.2-0.25%	Vinyl	0.25	1.40	12800	−126
DM441.2-0.50%	Vinyl	0.50	2.79	12800	−126
DM441.2-0.75%	Vinyl	0.75	4.19	12800	−126
DM441.2-1.00%	Vinyl	1.00	5.59	12800	−126
DM441.2-1.75%	Vinyl	1.75	9.80	12800	−126
DM441.2-2.50%	Vinyl	2.50	14.0	12800	−126
DM441.2-5.00%	Vinyl	5.00	27.9	12800	−125
DM441.2-100%	–	100.00	559	12900	−123

Ion conductivity of polymer systems

Ion conductivity (σ) in a single charge carrier system (such as the PDMS systems examined in this study) is given by:

$$\sigma = C_i q \mu \tag{3}$$

where C_i is the mobile ion concentration, q is the magnitude of the ion charges and μ is the mobility of the ions.

Since ion conductivity is a function of both mobile ion concentration and ion mobility, models describing ion conductivity are usually developed as the product of two quantities (as discussed in more detail in a previous publication[5]): an ion concentration factor and an ion mobility factor. The ion concentration factor is slightly dependent on temperature and reflects the ability of the polymer to solvate a salt into mobile ions. Thus, the effective mobile ion concentration is a function of the structure of the polymer, the structure of the salt and the concentration of mobile chain segments. The ion mobility factor is strongly temperature dependent and is a function of the size of the ion and the mobility of the polymer chain segments (since polymer chain segment motion is necessary for ion motion).

Because of the strong theoretical and experimental relationships between ion conductivity and viscosity[4,19–21], arguments similar to those used to describe the temperature dependence of chain segment mobility are used to describe the temperature dependence of ion mobility. Close to T_g ($T < T_g + 100°C$), insufficient free volume for movement leads to a decrease in chain segment mobility beyond simple Arrhenius behaviour. Thus, ion mobility should also decrease beyond simple Arrhenius behaviour, as the transport of ions strongly depends on the motion of polymer chain segments. A decrease in free volume may also lead directly to a decrease in ion mobility, if the ion itself is large enough to be limited in mobility by insufficient free volume for movement. Therefore, free volume type models are offered to describe ion motion in this temperature range. The types of models employed include semi-empirical WLF type expressions[22–35] and a modified Berry–Fox expression developed by Simpson and Bidstrup[4]. Because of the unique physical significance of its parameters, a modified Berry–Fox expression is applied in this research[5]:

$$\sigma = F'(C_i)\left\{\exp\left[\frac{B'}{f_g + (\alpha_1 - \alpha_0)(T - T_g)}\right]\right\}^{-1} \tag{4}$$

where $F'(C_i)$ is the ion concentration factor and B' is the fractional free volume required for ion motion (the free volume required for ion motion divided by the occupied chain segment volume). The ion concentration factor, $F'(C_i)$, is proposed to be directly related to mobile ion concentration (C_i). The ion mobility factor is equal to the exponential term in equation (4).

Far above T_g ($T > T_g + 100°C$), where a relatively large amount of free volume exists in the polymer system, the availability of free volume no longer limits chain segment or ion mobility. In this temperature range, an ion moves by overcoming an apparent activation energy. Therefore, Arrhenius type models are used to describe ion motion in this temperature region[25,26,35,36]:

$$\sigma = \sigma_\infty \exp\left(\frac{-E_\sigma}{RT}\right) \tag{5}$$

where σ_∞ is a pre-exponential factor (the ion concentration factor) and E_σ is the apparent energy of activation for ion motion (the ion mobility factor). The pre-exponential term (σ_∞) depends on the concentration of mobile ions in the polymer system. The activation energy (E_σ) is the energy required to move an ion from its position to an unoccupied position, and should include the energy required to move any chain segments necessary for ion motion.

Earlier[5], the free volume and Arrhenius ion conductivity models were shown to hold for the PDMS salt systems. The effects of ion size were evident in the best-fit model parameters E_σ and B'. E_σ increased in proportion to cation radius raised to the 0.27 power. B' also increased with ion size for the two cation systems (TPA^+ and TBA^+) that exhibited free volume type behaviour.

The effect of polymer chain length on ion conductivity was found to be related to the effect of the length of the mobile chain segment on ion conductivity[5]. As mobile chain segment length increased, the concentration of mobile ions (in a saturated system) decreased. Therefore, changes in the mobile chain segment length were apparent in the best-fit model parameters proposed to be related to mobile ion concentration (σ_∞ and $F'(C_i)$). As determined by these best-fit parameters, polymer solvation strength increased with mobile chain segment length raised to the -3.2 ± 0.6 power (σ_∞) or -2.3 ± 0.8 power ($F'(C_i)$).

In this investigation, the free volume (equation (4)) and Arrhenius (equation (5)) ion conductivity models will be applied to model the temperature dependence of the ion conductivity of the PDMS salt doped PDMS oils listed in *Table 1*. Differences in mobile ion concentration between samples should be reflected in differences in the best-fit model parameters proposed to be related to mobile ion concentration ($F'(C_i)$ and σ_∞).

EXPERIMENTAL

PDMS oil systems

The α,ω-divinyl and α,ω-trimethyl PDMSs used in this study were purchased from Hüls America, Inc. These samples were purified before use by dissolving in methylene chloride, drying over anhydrous magnesium sulfate, vacuum filtering (pore size 4–5.5 μm), rotary evaporating at 35°C, and storing under full vacuum at 35–40°C for 16 h.

PDMS salt systems

The α,ω-bis(γ-M-n-propyl-carboxylate) PDMSs (where M is a univalent cation, as shown in *Figure 1*) used in

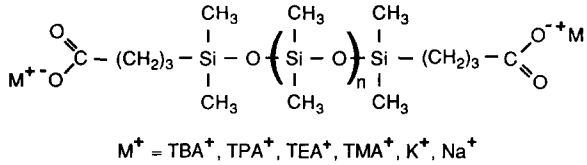

Figure 1 The structure of the PDMS salts used in this study where $M^+ = Na^+$, TMA^+ and TPA^+

this study were synthesized by neutralizing α,ω-bis(γ-n-propyl-carboxy) PDMSs with the appropriate hydroxide bases (M^+OH^-)[37]. The α,ω-bis(γ-n-propyl-carboxy) PDMSs were synthesized via a redistribution equilibration reaction between octamethylcyclotetrasiloxane and α,ω-bis(γ-n-propyl-carboxy) tetramethyl-disiloxane (both Hüls America, Inc.) in the presence of a sulfuric acid catalyst[38]. In this work, α,ω-bis(γ-M-n-propyl-carboxylate) PDMSs of the following cations were synthesized: Na^+, TMA^+ and TPA^+. These polymers were purified before use in the same manner as the α,ω-divinyl and α,ω-trimethyl PDMSs.

PDMS salt doped PDMS oil systems

Each PDMS salt doped PDMS oil sample examined in this study was prepared by mixing a α,ω-bis(γ-M-n-propyl-carboxylate) PDMS with a α,ω-divinyl or α,ω-trimethyl PDMS of the same chain length, as detailed below. First, an oil and salt were combined in amounts determined to yield complexes with the desired doping level of salt. Then, this sample was diluted in methylene chloride (in order to improve the oil and salt mixing) and magnetically stirred at room temperature for 12–16 h. A typical sample consisted of 10 g total PDMS polymers in 100 ml methylene chloride. Finally, the sample was purified before use by drying over anhydrous magnesium sulfate, vacuum filtering (pore size 4–5.5 μm), rotary evaporating at 35°C, and storing under full vacuum at 35–40°C for 16 h. In this investigation, PDMS salts of univalent cations, $M = Na^+$, TMA^+ and TPA^+, were doped into PDMS oils, in the amounts delineated in *Table 1*. The mole per cent cations in each sample was calculated (per unit volume) as the number of cations divided by the total number of main chain units ($Si(CH_3)_2$–O counting as two main chain units) times 100%.

Nuclear magnetic resonance

The structure of each PDMS sample was verified by ^1H n.m.r. These spectra were obtained on a Varian XL-400 Nuclear Magnetic Resonance Spectrometer, using the undeuterated fraction of the methylene chloride solvent as an internal standard (chemical shift (δ) = 5.32 ppm).

Gel permeation chromatography

The weight-average molecular weight (M_w) of each PDMS sample was determined by g.p.c. Analyses were performed at 35°C using a Waters Liquid Chromatograph System equipped with a Waters model 410 Differential Refractometer Detector and three Phenomenex Phenogel 5 g.p.c. columns (10^3 Å, 10^4 Å and 10^5 Å). Toluene was used as the carrier solvent. For the sake of comparison, the average molecular weights reported in *Table 1* are the average molecular weights of the samples minus the relative contributions of the different cation end groups.

Differential scanning calorimetry

The T_g of each PDMS sample was measured on a Seiko Instruments DSC220C Automatic Cooling Differential Scanning Calorimeter. A heating rate of 10°C min^{-1} was used. The T_g was taken as the midpoint of the change in heat capacity associated with T_g. The T_g of each PDMS sample is reported in *Table 1*.

Dilatometry

A Perkin–Elmer Series 7 Thermomechanical Analysis System equipped with the extension probe and the dilatometer accessory was used to measure the temperature-dependent volumetric thermal expansion coefficient of each PDMS sample over the range −50°C to 70°C.

Rheology

A Bohlin Instruments VOR Rheometer was used to measure the zero-shear viscosity of each PDMS sample over the temperature range −50°C to 65°C. The rheometer was equipped with the Fluids Head Option and the Low Temperature Measurement Option. Measurements were made using a parallel plate geometry consisting of a 25 mm upper plate and a 40 mm lower plate. The larger lower plate was used to ensure the correct edge profile for the low viscosity liquids studied. Thermal expansion of the test fixtures was accounted for in order to maintain a constant gap between the plates. At each temperature, the steady-shear viscosity of each sample was measured over a possible shear rate range of 3.37×10^{-3} to 2.65×10^3 s^{-1}. The zero-shear vicosity was defined as the average steady-shear viscosity, when the steady-shear viscosity remained constant (Newtonian) over two decades of shear rates.

Dielectrometry

A Micromet Instruments Eumetric System III Microdielectrometer was used to determine the ion conductivity of each PDMS sample over the temperature range −45°C to 60°C. The microdielectrometer was equipped with the Low Conductivity Measurement Option and disposable 14 inch Low Conductivity Integrated Circuit Sensors. Temperature cycling was performed in a Fisher Scientific Isotemp Vacuum Oven (model 281A) for temperatures above room temperature. For sub-ambient temperature measurements, a thermoelectric heating/cooling module (Tellurex Corp.) with a dry-ice cold sink was used. At each temperature, the loss factor, $\varepsilon''(\omega)$, was measured over a frequency range of 0.1–10 000 Hz. The loss factor, $\varepsilon''(\omega)$, is a measure of the energy required for molecular motion in the presence of an electric field. It consists of energy losses due to the orientation of molecular dipoles, $\varepsilon_d''(\omega)$, and energy losses due to the conduction of ionic species, $\varepsilon_c''(\omega)$:

$$\varepsilon''(\omega) = \varepsilon_d''(\omega) + \varepsilon_c''(\omega) \tag{6}$$

Based on Debye's model of dipolar behaviour[39], $\varepsilon_d''(\omega)$ is a complex function of the relaxation time and the measurement frequency. The energy loss due to the conduction of ions, $\varepsilon_c''(\omega)$, is simply inversely proportional to frequency and equal to $\sigma/\omega\varepsilon_0$. Equation (6) can then be written:

$$\varepsilon''(\omega) = \varepsilon_d''(\omega) + \frac{\sigma}{\omega\varepsilon_0} \tag{7}$$

where ε_0 is the permittivity of free space equal to 8.85×10^{-14} F cm^{-1}. The dielectric loss factor is therefore dominated by energy losses due to ion conduction where $\varepsilon''(\omega)$ exhibits a linear dependency with $1/\omega$. The ion conductivity was thus defined as the average ion conductivity calculated from the loss factor, when the

ion conductivity exhibited a linear dependency with $1/\omega$ over two decades of frequency.

All of the ion conductivities reported in this paper are at least one order of magnitude above the lower limit of sensitivity of the sensors used (10^{-14} to 10^{-15} S cm^{-1}, varying from sensor to sensor).

Error analysis

The uncertainty in any data presented in this paper was calculated for a 90% confidence interval, assuming a Student's t distribution of the data.

RESULTS AND DISCUSSION

Viscosity of PDMS salt doped PDMS oils

The zero-shear-rate viscosity of each PDMS salt doped PDMS oil was measured over the temperature range $-50°C < T < 60°C$. The lower measurement temperature limit was fixed at approximately $-50°C$, as this is the temperature at which these PDMS samples crystallize.

The temperature-dependent zero-shear-rate viscosities of the doped samples were identical to those of pure PDMS oils of the same chain length, within experimental uncertainty[40] (e.g. the DM438 samples shown in *Figure 2*). The M_w, T_g and α_1 values of the doped samples were also statistically identical to those of undoped oils of the same chain length[5]. Therefore, the Arrhenius and free volume viscosity model best-fit parameters previously determined for the oils[5] also represent doped samples of the same chain length. To recapitulate these results, in PDMS systems, both E_η (Arrhenius model) and B (free volume model) increase with chain length and then level off to constant values at a chain length of about 140 main chain atoms ($M_w = 5190$). This means that the length of the characteristic unit of flow (i.e. the length of the mobile polymer chain segment) in PDMS systems increases with chain length and levels off at a chain length of about 140 main chain atoms. Also, f_g increases with chain length and levels off to a value of 0.034 at $M_w = 5190$.

Ion conductivity of PDMS salt doped PDMS oils

The effects of salt concentration on ion conductivity for three of the nine molecular weight–cation combinations studied are shown in *Figures 3–5*. So as not to

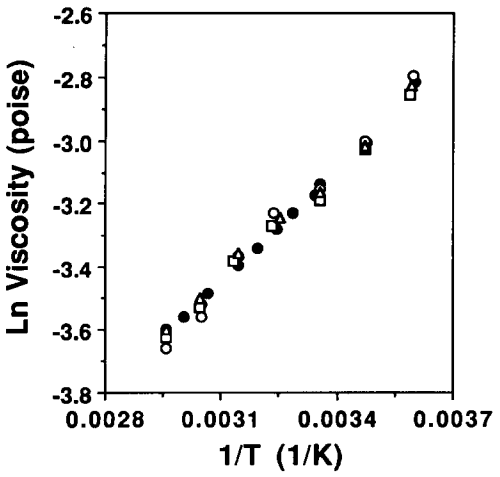

Figure 2 Temperature dependence of the viscosity of PDMS M^+ salt doped PDMS oils of $M_{w,oil} = 1200$. ●, DM438-0% (pure oil); ○, DTPA438-5.00%; □, DTMA438-5.00%; △, DNa438-2.50%

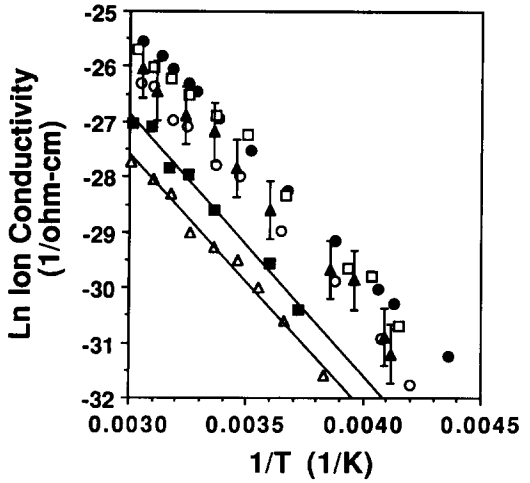

Figure 3 Temperature dependence of the ion conductivity of PDMS Na^+ salt doped PDMS oils of $M_{w,oil} = 1200$. Solid lines represent Arrhenius model predictions (equation (5)) in the temperature range $-45°C < T < 60°C$. ●, DNa438-100%; ○, DNa438-2.50%; □, DNa438-1.00%; ▲, DNa438-0.50%; ■, DNa438-0.25%; △, DNa438-0.10%

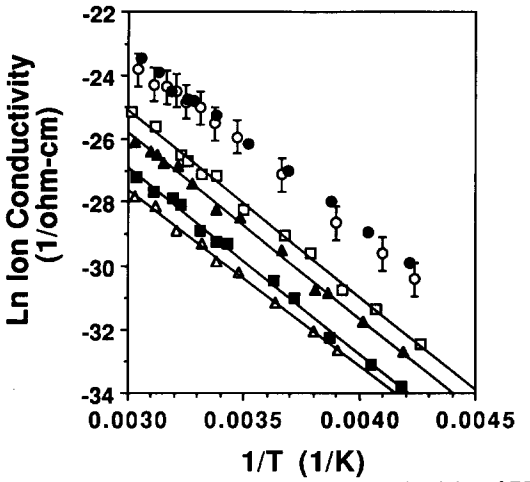

Figure 4 Temperature dependence of the ion conductivity of PDMS TMA^+ salt doped PDMS oils of $M_{w,oil} = 1200$. Solid lines represent Arrhenius model predictions (equation (5)) in the temperature range $-45°C < T < 60°C$. ●, DTMA438-100%; ○, DTMA438-5.00%; □, DTMA438-2.50%; ▲, DTMA438-1.00%; ■, DTMA438-0.50%; △, DTMA438-0.10%

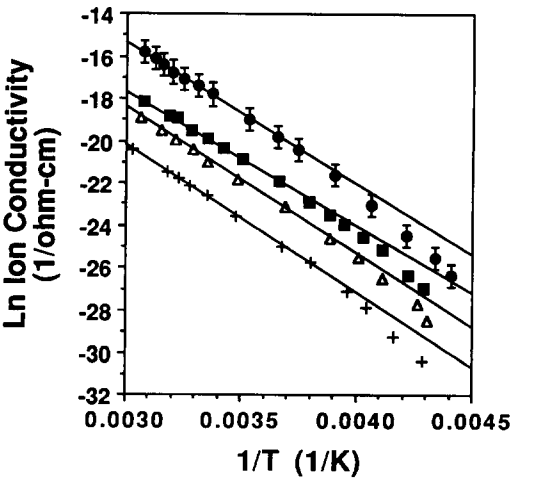

Figure 5 Temperature dependence of the ion conductivity of PDMS TPA^+ salt doped PDMS oils of $M_{w,oil} = 2720$ over the temperature range $-45°C < T - T_g < 60°C$. Solid lines represent Arrhenius model predictions (equation (5)) in the temperature range $-15°C < T < 60°C$. ●, DTPA039.5-100%; ■, DTPA039.5-1.00%; △, DTPA039.5-0.50%; +, DTPA039.5-0.10%. The data for DTPA039.5-5.00%, DTPA039.5-2.50% and DTPA039.5-1.75% were statistically identical to DTPA039.5-100%

complicate these figures any further, error bars are shown on only one set of data on each figure. However, the uncertainty in ln σ is the same for each set of data (± 0.53). The solid lines in each figure represent the best fits of Arrhenius models (equation (5)) through the data in the temperature range $-15°C < T < 60°C$. In the cases of the series of doped samples of the two smaller cations (DM438-X%, DM039.5-X% and DM441.2-X%, where M = Na^+ or TMA^+ and X% = wt% salt), Arrhenius models were actually fitted through the data over the entire temperature range ($-45°C < T < 60°C$), as these data do not exhibit free volume type curvature for $T < -25°C$. However, the data for the TPA^+ doped samples (DTPA438-X%, DTPA039.5-X% and DTPA441.2-X%) do exhibit free volume type curvature in the temperature range $-50°C < T < -20°C$. Therefore, the ion conductivity data of the TPA^+ salt doped samples were fitted with free volume models (equation (4)) in this temperature region. An example of the free volume model fits for one of these TPA^+ series is shown in *Figure 6*. The average best-fit Arrhenius (σ_∞ and E_σ) and free volume ($F'(C_i)$ and B') ion conductivity model parameters for all of the doped samples examined are presented in *Tables 2–4*. $F'(C_i)$ and B' are the only fitted parameters in the free volume model, since M_w, α_1 and T_g were measured for each sample, α_0 was assumed to equal zero, and f_g was determined to be 0.034 from the free volume viscosity model[5].

Again, ion conductivity is a function of both ion mobility and mobile ion concentration. For a particular doped oil series (e.g. DTPA039.5-X%), ion mobility is constant, as both the size of the ion and the size of the mobile chain segment are constant. The concentration of mobile chain segments, the solvation strength of these segments and the strength of the salt are also constant. Therefore, any differences in ion conductivities between samples in a doped oil series are due to differences in the

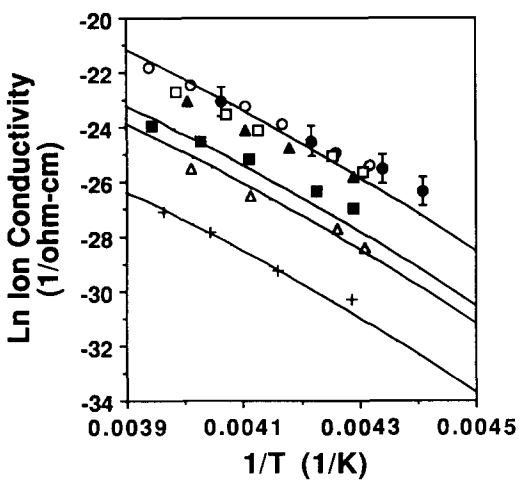

Figure 6 Temperature dependence of the ion conductivity of PDMS TPA^+ salt doped PDMS oils of $M_{w,oil} = 2720$. Solid lines represent free volume model predictions (equation (4)) in the temperature range $-45°C < T < -20°C$. ●, DTPA039.5-100%; ○, DTPA039.5-5.00%; □, DTPA039.5-2.50%; ▲, DTPA039.5-1.75%; ■, DTPA039.5-1.00%; △, DTPA039.5-0.50%; +, DTPA039.5-0.10%

Table 2 Arrhenius (equation (5)) ion conductivity model best-fit parameters for the PDMS Na^+ salt doped PDMS oils

	Arrhenius model	
	ln σ_∞ (S cm^{-1})	E_σ (kcal mol^{-1})
DNa438-0.10%	-13.71 ± 0.53	9.0 ± 0.2
DNa438-0.25%	−12.62	9.0
DNa438-0.50, 1.00, 100%	−12.06	9.0
DNa039.5-0.10%	No data	No data
DNa039.5-0.25, 0.50, 1.00, 100%	−13.46	9.0
DNa441.2-0.10%	No data	No data
DNa441.2-0.25, 0.50, 1.00, 2.50, 100%	−15.38	9.0

Table 3 Arrhenius (equation (5)) ion conductivity model best-fit parameters for the PDMS TMA^+ salt doped PDMS oils

	Arrhenius model	
	ln σ_∞ (S cm^{-1})	E_σ (kcal mol^{-1})
DTMA438-0.10%	-11.01 ± 0.53	11.4 ± 0.2
DTMA438-0.50%	−9.28	11.4
DTMA438-1.00%	−8.36	11.4
DTMA438-2.50%	−7.65	11.4
DTMA438-5.00, 100%	−6.90	11.4
DTMA039.5-0.10%	−11.74	11.4
DTMA039.5-0.50%	−10.03	11.4
DTMA039.5-0.75, 1.00, 100%	−8.64	11.4
DTMA441.2-0.10%	−16.25	11.4
DTMA441.2-0.50%	−14.71	11.4
DTMA441.2-0.75, 1.00, 2.50, 5.00, 100%	−11.43	9.0

Table 4 Arrhenius (equation (5)) and free volume (equation (4)) ion conductivity model best-fit parameters for the PDMS TPA^+ salt doped PDMS oils

	Arrhenius model		Free volume model	
	ln σ_∞ (S cm^{-1})	E_σ (kcal mol^{-1})	ln $F'(C_i)$ (S cm^{-1})	B'
DTPA438-0.10%	2.04 ± 0.53	13.7 ± 0.2	-9.28 ± 0.53	2.6 ± 0.2
DTPA438-1.00%	4.12	13.7	−7.07	2.6
DTPA438-2.50%	4.52	13.7	−5.05	2.6
DTPA438-5.00, 10.0, 100%	6.18	13.7	−5.89	2.6
DTPA039.5-0.10%	0.59	13.7	−11.33	2.7
DTPA039.5-0.50%	2.18	13.7	−8.83	2.7
DTPA039.5-1.00%	2.98	13.7	−8.37	2.7
DTPA039.5-1.75, 2.50, 5.00, 100%	4.78	13.7	−6.34	2.7
DTPA441.2-0.10%	−9.00	13.7	−16.80	3.1
DTPA441.2-0.50%	−6.92	13.7	−14.90	3.1
DTPA441.2-1.00%	−3.73	13.7	−11.71	3.1
DTPA441.2-1.75, 2.5, 100%	−1.96	13.7	−9.91	3.1

number of mobile ions doped into these systems (i.e. differences in mobile ion concentration). Moreover, ion conductivity should decrease directly with a decrease in mobile ion concentration (see equation (3)).

Within each doped oil series, the temperature-dependent ion conductivities are statistically similar for relatively large amounts of salt (e.g. 100 wt% to 1.75 wt% in the DTPA039.5-X% systems). For lower amounts of salt (e.g. 1.00 wt% to 0.10 wt% in the DTPA039.5-X% systems), the ion conductivities decrease with a decrease in salt concentration. Therefore, these PDMS systems must be saturated with mobile ions at the higher salt concentrations. When the temperature-dependent ion conductivities of these samples drop below the values of the 100 wt% salt system, this indicates that these systems are no longer saturated with mobile ions.

In the discussion that follows, the mole percentage of cations in each sample (see *Table 1*) is used as a relative measure of cation concentration. The saturation mobile ion concentration for each doped series is estimated as an average between the ion concentration before which a statistically significant decrease in the temperature-dependent ion conductivity is first observed and the ion concentration of the sample in which the decrease is first observed. For example, ion conductivity drops off between DTPA039.5-1.75% (0.042 mol% cations) and DTPA039.5-1.00% (0.024 mol% cations) in *Figure 5*. Therefore, the approximate saturation ion concentration is defined as 1.37 wt% (0.33 mol% cations) for the DTPA039.5-X% series.

The best-fit parameters of both the Arrhenius and free volume models can be used to gain a better, quantitative understanding of the effects of mobile ion concentration on the ion conductivity of polymers, as illustrated by the application of these models to these PDMS systems. The component of the Arrhenius model dependent on the number of mobile ions in the system is the pre-exponential term (σ_∞), which is proposed to be directly related to mobile ion concentration. As noted previously[5], σ_∞ is a useful measure of relative mobile ion concentration only in systems with the same mobile ions,

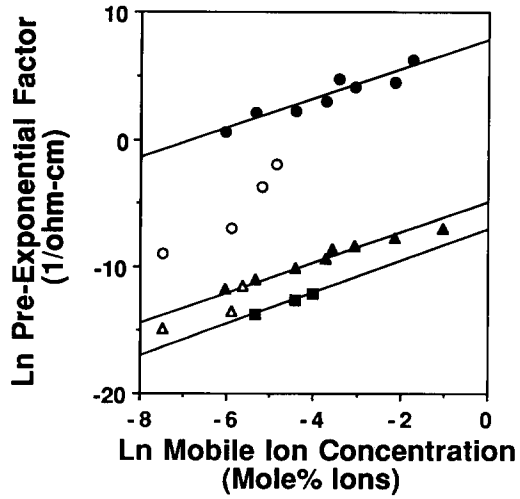

Figure 7 The Arrhenius ion conductivity model pre-exponential factor (σ_∞) as a function of relative mobile ion concentration for the PDMS salt doped PDMS oils. ●, DTPA438-K% and DTPA039.5-K% samples; ○, DTPA441.2-K% samples; ▲, DTMA438-K% and DTMA039.5-K% samples; △, DTMA441.2-K% samples; ■, DNa438-K% samples

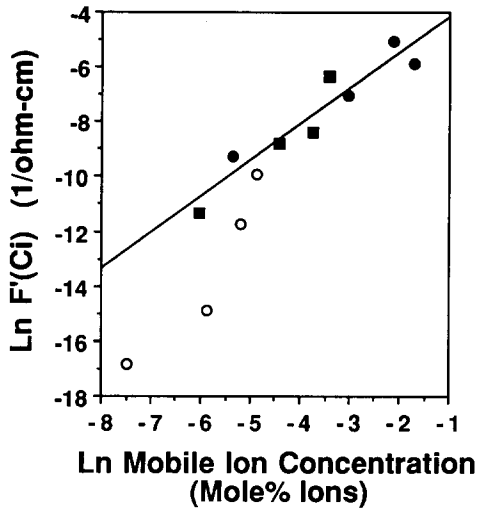

Figure 8 The free volume ion conductivity model mobile ion concentration factor ($F'(C_i)$) as a function of relative mobile ion concentration for the PDMS TPA^+ salt doped PDMS oils. ●, DTPA438-K% samples; ■, DTPA039.5-K% samples; ○, DTPA441.2-K% samples

and cannot be used to compare the relative mobile ion concentrations of systems with different size cations. If σ_∞ is directly related to mobile ion concentration, then a log–log plot of σ_∞ *versus* mol% mobile cations for samples of the same cation should yield a straight line with a slope of 1.0.

In *Figure 7*, σ_∞ is shown as a function of relative mobile ion concentration for systems of each of the three cations studied. A straight line is fitted through the DM438-X% and DM039.5-X% data of each cation (the higher mobile ion concentration data points). The average slope of these lines is 1.1 ± 0.1, which is within experimental uncertainty of the theoretical value of 1.0. However, this relationship appears to fall apart for the DM441.2-X% data. The DTPA441.2-X% data have a slope of 2.5 and the DTMA441.2-X% data have a slope of 2.0. At present, no explanation for the failure of the model in the cases of these samples can be offered. Therefore, a conclusion as to the validity of σ_∞ as a measure of mobile ion concentration is mixed: it appears to be a very good measure of relative mobile ion concentration in same-ion systems of relatively high mobile concentration (>0.006 mol%), but a poor measure of ion concentration in systems of relatively low mobile ion concentration (<0.006 mol%).

The component of the free volume model dependent on the number of mobile ions in the system is the pre-exponential term ($F'(C_i)$), which is also proposed to be directly related to mobile ion concentration. Analogous to σ_∞, $F'(C_i)$ is useful only in comparing the relative mobile ion concentrations of systems with the same mobile ions[5]. If $F'(C_i)$ is directly related to mobile ion concentration, then a log–log plot of $F'(C_i)$ *versus* mobile ion concentration should also yield a straight line with a slope of 1.0.

In *Figure 8*, $F'(C_i)$ is shown as a function of relative mobile ion concentration. A straight line is fitted through the data of the DTPA438-X% and DTPA039.5-X% samples. The slope of this line is 1.3 ± 0.3, which is within experimental uncertainty of the theoretical value of 1.0. However, this relationship does not seem to hold for the DTPA441.2 data. The DTPA441.2-X% data have a slope of 2.5. Again, as in the case of σ_∞ in the Arrhenius model,

no explanation can be offered for the failure of this parameter in systems of relatively low mobile ion concentration. Therefore, a conclusion as to the validity of the $F'(C_i)$ parameter as a measure of mobile ion concentration is also mixed: it appears to be an acceptable measure of relative mobile ion concentration in same-ion systems of relatively high mobile ion concentration (>0.006 mol%), but an unacceptable measure of ion concentration in systems of relatively low mobile ion concentration (<0.006 mol%).

The other best-fit parameters in the ion conductivity models are E_σ (Arrhenius) and B' (free volume), which are dependent on ion mobility (i.e. ion size and mobile chain segment length) and independent of mobile ion concentration. Therefore, no change in these parameters with mobile ion concentration is seen in *Tables 2–4*. The values of E_σ and B' reported in these tables are in agreement with the values reported earlier for pure Na^+, TMA^+ and TPA^+ salt systems only[5].

CONCLUSIONS

Depending on the temperature range, the zero-shear-rate viscosities of the PDMS salt doped PDMS oils examined in this study were successfully described by either Arrhenius ($100°C < T - T_g < 185°C$) or free volume ($100°C < T - T_g < 185°C$) models. Moreover, the temperature-dependent viscosities, M_w, T_g and α_1 values of the doped samples were identical to those of undoped oil samples of the same chain length. Therefore, the best-fit model parameters of these doped samples, and conclusions regarding the flow characteristics of these samples, are the same as those previously reported for the undoped PDMS oils[5].

The effects of mobile ion concentration on ion conductivity in polymer systems of the same mobile cation are reflected in the best-fit model parameters σ_∞ (in the Arrhenius model) and $F'(C_i)$ (in the free volume model). As proposed, both of these parameters are directly proportional to mobile ion concentration raised to the 1.0 power (within experimental uncertainty), but only for relatively high mobile ion concentrations (>0.006 mol%). For low amounts of mobile ions (<0.006 mol%), this relationship appears to fail, as these parameters appear to be proportional to mobile ion concentration raised to the 2.0 or 2.5 power.

ACKNOWLEDGEMENTS

The authors gratefully acknowledge Dr Charles Liotta for his assistance in developing the PDMS salt synthesis route; Dr Leslie Gelbaum for performing the n.m.r. measurements; Ms Natascha Azzolin, Mr Dan Klask and Mr Frank Lin for laboratory work assistance; Micromet Instruments for an equipment grant; and the Georgia Tech Manufacturing Research Center, the National Science Foundation (ECS-9058560), B. F. Goodrich and the Alcoa Foundation for their financial support.

REFERENCES

1 Wong, C.P. *Adv. Polym. Sci.* 1988, **84**, 63
2 Ratner, M. A. and Shriver, D. F. *MRS Bull.* 1989, (**Sept.**), 39
3 Senturia, S. D. and Sheppard, N. F. *Adv. Polym. Sci.* 1986, **80**, 1
4 Simpson, J. O. and Bidstrup, S. A. *J. Polym. Sci.: Part B: Polym. Phys.* 1993, **31**, 609
5 Companik, J. E. and Bidstrup, S. A. *Polymer* 1994, **35**, 4823
6 Berry, G. C. and Fox, T. G. *Adv. Polym. Sci.* 1968, **5**, 261
7 O'Conner, K. M. and Scholsky, K. M. *Polymer* 1989, **30**, 461
8 Lomellini, P. *Polymer* 1992, **33**, 4983
9 Doolittle, A. K. *J. Appl. Phys.* 1951, **22**, 1031
10 Doolittle, A. K. *J. Appl. Phys.* 1951, **22**, 1471
11 Doolittle, A. K. *J. Appl. Phys.* 1952, **23**, 236
12 Ferry, J. D. 'Viscoelastic Properties of Polymers', 3rd edn, John Wiley and Sons, New York, 1980, p. 287
13 Kumar, N. G. *J. Polym. Sci.: Macromol. Rev.* 1980, **15**, 255
14 Bueche, F. *J. Chem. Phys.* 1952, **20**, 1959
15 Ewell, R. H. and Eyring, H. *J. Chem. Phys.* 1937, **5**, 726
16 Rosevare, W. E., Powell, R. E. and Eyring, H. *J. Appl. Phys.* 1941, **12**, 669
17 Dodgson, K., Bannister, D. J. and Semlyen, J. A. *Polymer* 1980, **21**, 663
18 Billmeyer, F. W. 'Textbook of Polymer Science', 2nd edn, John Wiley and Sons, New York, 1984, p. 303
19 Kienle, R. H. and Race, H. H. *Trans. Electrochem. Soc.* 1934, **65**, 87
20 Lawless, G. W. *Polym. Eng. Sci.* 1980, **20**, 546
21 Kranbuehl, D. E. *J. Non-Crystalline Solids* 1991, **131–133**, 930
22 Ratner, M. A. *Mater. Forum* 1991, **15**, 1
23 Papke, B. L., Ratner, M. A. and Shriver. D. F. *Electrochem. Soc.* 1982, **129**, 1434
24 Watanabe, M. and Ogata, N. *Br. Polym. J.* 1988, **20**, 181
25 Killis, A., LeNest, J., Cheradame, H. and Gandini, A. *Makromol. Chem.* 1982, **183**, 2835
26 Berthier, C., Gorecki, W., Minier, M., Armand, M. B., Chabagno, J. M. and Rigaud, P. *Solid State Ionics* 1983, **11**, 91
27 Sheppard, N. F. PhD Thesis, Massachusetts Institute of Technology, 1986, p. 239
28 Adamic, K. J., Greenbaum, S. G., Wintersgill, M. C. and Fontanella, J. J. *J. Appl. Phys.* 1986, **60**(4), 1342
29 Martin, G. C., Tungare, A. V. and Gotro, J. T. *Proc. Am. Chem. Soc. Div. Polym. Mater.: Sci. Eng.* 1988, **59**, 980
30 Kranbuehl, D., Delos, S., Hoff, M., Weller, L., Haverty, P. and Seely, J. *Am. Chem. Soc. Symp. Ser.* 1988, **367**, 100
31 Bidstrup, S. A., Sheppard, N. F. and Senturia, S. D. *Polym. Eng. Sci.* 1989, **29**(5), 325
32 Xu, K., Wan, G. and Tsuchida, E. *Polym. Adv. Technol.* 1992, **3**, 67
33 Kim, D., Ryoo, B., Maeng, K. and Hwang, T. *Polym. J.* 1992, **24**(6), 509
34 Lane, J. W., Khattak, R. K. and Dusi, M. R. *Polym. Eng. Sci.* 1989, **29**, 339
35 Rietman, E. A., Kaplan, M. L. and Cava, R. J. *Solid State Ionics* 1985, **17**, 67
36 Munshi, M. Z. A. and Owens, B. B. *Polym. J.* 1988, **20**(7), 577
37 Companik, J. E. PhD Thesis, Georgia Institute of Technology, 1993, p. 37
38 Kojima, K., Gore, C. R. and Marvel, C. S. *J. Polym. Sci. A1* 1966, **4**, 2325
39 Debye, P. 'Polar Molecules', The Chem. Cat. Co., New York, 1929, p. 106
40 Companik, J. E. PhD Thesis, Georgia Institute of Technology, 1993, p. 97